



Journal of Applied Sciences

ISSN 1812-5654

science
alert

ANSI*net*
an open access publisher
<http://ansinet.com>

Beam Profile and Image Transfer Study in Multimode Optical Fiber Coupling

¹A. Asadpour and ²H. Golnabi

¹Plasma Physics Research Center, Islamic Azad University,
P.O. Box 14665-678, Tehran, Iran

²Institute of Water and Energy, Sharif University of Technology,
P.O. Box 11365-8639, Tehran, Iran

Abstract: In this study the optical beam transfer and imaging in an optical fiber coupling is discussed. In coupling two fibers, some measurements from intensity perspective are performed and intensity profile is investigated. A theoretical model for the power transmission in fiber coupling is developed and theoretical function is compared with the experimental results. The amount of light delivered to the receiving fiber depends on the acceptance angle of the receiving fiber and the core cross sections of both fibers. Intensity profile function obtained theoretically agrees well with the measured results. The intensity variation as a function of the air gap variation is investigated in this article. The image of emerging beam of the source fiber is also investigated. Using captured images one can measure acceptance angle and core diameter of the fiber by using two images of the output beam at two axial distances. The results of this report can be used in optical communications, data links and image transferring in which single or coupled optical fibers have been used as signal carrier or waveguide.

Key words: Fiber optics, fiber splice, image transfer, axial coupling

INTRODUCTION

A multimode fiber can be used as a waveguide for lighting and transmission of optical energy of a light source in scientific, medical, industrial or other applications. The beam shape of the transmitted power can be therefore very important in such applications depending on the required beam specification (Ersoy, 2007). Beam power measurements and profiling make it possible to directly check the fiber waveguide beam profile and mode characteristics. It is also possible to look at the emerging light beam from the beam shaping optics following the guiding fiber. Such monitoring verifies that whether all the related optical/electro-optical components are performing as expected and be able to make real-time adjustments for the precise and optimum performance. For flow cytometry, for instance, it is necessary to create a flat-topped beam to provide uniform illumination of the flow cell.

Fiber splicing is a coupling technique by which the cut ends of two optical fibers can be attached together, resulting in nearly a single piece of long fiber optical transmission line (Senior, 1992). Because of the mentioned importance, experimental study of the beam profile variation in a fiber splicing joint is presented in this report.

Moreover we take a brief look at the developed theoretical formulations in beam transmission and image information in fibers and fiber coupling.

Our expectation is that obtained results could shed some light on the case of optimum parallel energy transfer in fibers/fiber bundles and higher optical bandwidth could be resulted for data links in communication (Raddatz *et al.*, 1998). Information about image and power distribution in a fiber or fiber splice joint can also provide information about the uniformity of the transmitted light beam profile (Tsekrekos *et al.*, 2007). In this study the theory of power transfer in multimode fiber coupling is developed and we try to formulate a transfer function for the implemented multimode plastic optical fibers.

MATERIALS AND METHODS

This study was conducted in Institute of Water and Energy a research center of Sharif University of Technology during period of 2006-2008. Transmitted power distribution in a fiber splice joint has been investigated in many references (Fujii *et al.*, 1984; Cherin and Rich, 1978) and different fiber splice connectors have been designed in order to reduce transmitted power loss. Fiber bundles as well as single

fiber line can be used for image transmittance in optical apparatus and different types of connectors have been designed for this objective (Ren *et al.*, 2001). As shown in Fig. 1, a low power incandescent white lamp illuminates the source fiber; receiving fiber fixed on a 3D-translational stage is aligned with the source fiber using the micrometer stage and the emerging light from the receiving fiber is measured by a power meter. In this study we have used 40 cm long plastic multimode optical fibers as the source and receiving fibers with an overall diameter of 2 mm including core, cladding plus core diameter of 980 μm and the protective sleeve. The nominal core diameter of this fiber is about 860 μm (99%) of the whole diameter. Index of refraction of the core for a typical plastic fiber is $n_1 = 1.45$ and the cladding $n_2 = 1.44$, which results a Numerical Aperture (NA) of about 0.17.

By monitoring output transmitted power the case of the maximum transmitted power is obtained for the best x-and y-alignment for a given axial gap separation, z. The variation of optical power by any misalignments in x and y directions can be obtained using the related micrometers and power recording (Fig. 1). It is also possible to consider the variation of the transmitted power as a function of the axial distance, z, in such

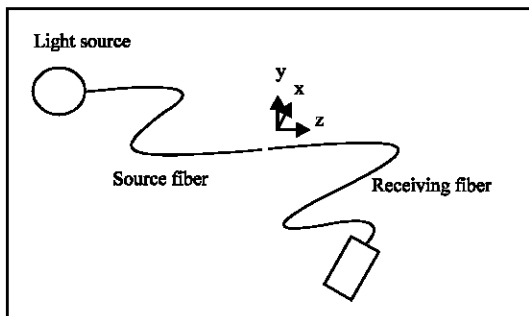


Fig. 1: Set up for transmitted power measurement

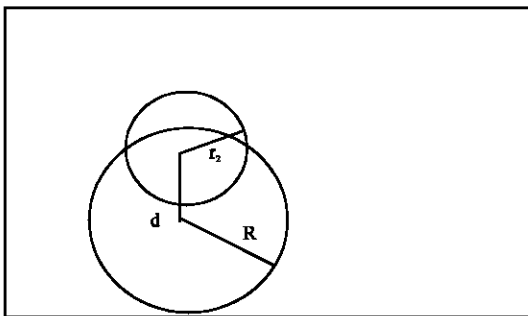


Fig. 2: Intersection of the receiving fiber cross section (top circle) and emerging beam cross section (bottom circle)

coupling. Typical axial gap separation is in the range of 0.01 mm to 1 mm and offset variation range of the receiving fiber (fixed to the translational stage) is on the order of the fiber core diameter.

The theoretical model for the intensity/power transmission can be derived from the geometrical optics by considering the beam cross sectional intersections. If we assume a cone of light emerging from the source fiber then the amount of light delivered to the receiving fiber depends on the acceptance angle of the receiving fiber or the core cross section of such fiber. Thus we consider such light acceptance cone by the overlap of the base cone of the emerged light from the source and the cross section circle of the receiving fiber. The circular cross sections and the overlap intersections are indicated in Fig. 2. Using the intersection of the areas of receiving fiber and the base of the emerging cone light we can determine the transmitted intensity variation.

In the case of x-y offset misalignment, the overlap area of two circles can be expressed by the following piecewise functions:

$$\Delta S(d) = \begin{cases} \pi r_2^2 & d < R - r_2 \\ \pi r_2^2 - (\arcsin(\frac{y}{r_2})r_2^2 - (\arccos(\frac{y}{R})R^2 - dy)) & R - r_2 < d < R \\ \arcsin(\frac{y}{R})R^2 + \arcsin(\frac{y}{r_2})r_2^2 - dy & R - r_2 < d < R + r_2 \\ 0 & d > R + r_2 \end{cases}$$

$$y = \sqrt{r_2^2 - \frac{1}{4d^2}(r_2^2 - R^2 + d^2)^2}$$

(1)

in which R is the radius of cone base of the emerging beam, r_2 is the core radius of receiving fiber and d is the distance between the fiber beam image circle (R) and receiving fiber core centers. It must be pointed out that the value of R is given by

$$R = r_1 + z \tan \theta$$

(2)

where, θ is the acceptance angle of the cone light, r_1 is the core radius of the source fiber and z is the axial distance. The minimum cross section is zero and the maximum cross section is equal to the cross section of the receiving fiber according to Eq. 1. For the case of similar source and receiving fibers we have $r_1 = r_2$. Similar to our recent report on double fibers (Golnabi and Azimi, 2008) the variation of the received intensity depends on the beam overlap cross section.

To study intensity profile and transmitted image of the source fiber a CCD camera is used in experimental arrangement of Fig. 1, instead of the power meter just

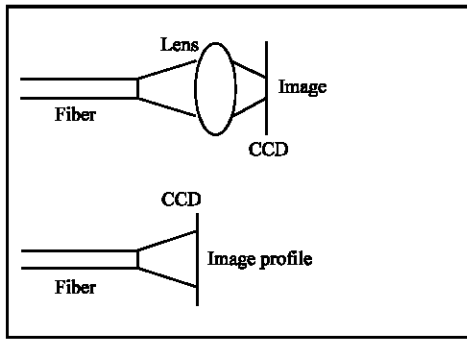


Fig. 3: Arrangement for the image and intensity profile measurements

behind the source fiber. CCD cameras are used widely for image capturing and designing vision systems in different applications (Zhang *et al.*, 2005). As shown in Fig. 3, for image recording the focusing lens is placed in position and for intensity distribution experiments when intensity profile is required the focusing lens in front of the CCD camera is removed.

RESULTS AND DISCUSSION

Using the mentioned methods experimental results concerning optical fiber coupling are described in this section. Results include intensity preview of the transmitted intensity and also the image analysis. The measured intensity scans as a function of the x-and y-variations are shown in this section. Figure 4 shows the power variation as a function of x distance. In such experiments two fibers have a longitudinal air gap distance of about $z = 0.01$ mm. As shown in Fig. 4, the output intensity starts at 0.52 nW level and decreases to about 0.02 nW for an axial separation of about 0.9 mm. By increasing more axial separation the output power is almost constant, which is just the output due to background signal (stray light and detector dark noise). As can be seen in Fig. 4, decrease as a function of x value is nearly linear with a rate of about 0.55 nW/mm.

In Fig. 5, the output power variation as a function of y scan is displayed. As can be shown in Fig. 5, transmitted power is decreasing by increasing y value. Such decrease is almost linearly and continues until an offset y value of about 0.9 mm. From this point the transmitted power is almost constant, which agrees with overlap cross section given by Eq. 1 for the case of $d > R+r_2$. Theoretical calculation estimates that transmitted power should drop to zero at this point, but experimental value shows a small value because of the background signal.

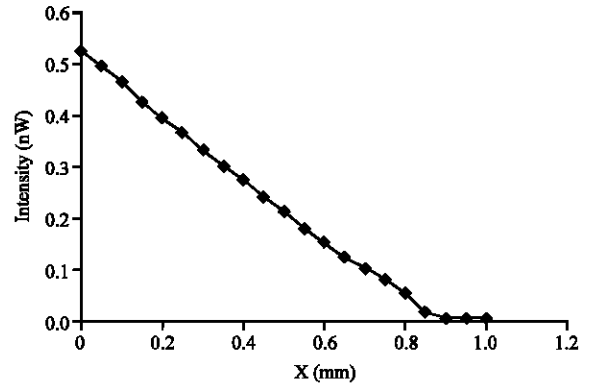


Fig. 4: Intensity variation in receiving fiber in x-scan ($z = 0.01$ mm, $y = 0$)

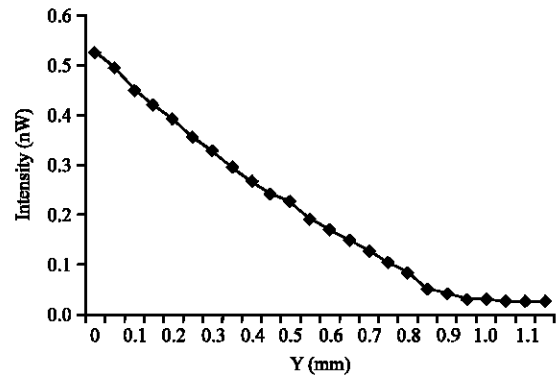


Fig. 5: Intensity variation in receiving fiber in y-scan ($z = 0.01$ mm, $x = 0$)

As expected because of the symmetry transmitted power for y-offset should be the same as x-offset results. The transmitted power is changing nearly linearly and start from 0.52 nW and drops to a value of about 0.05 nW (Fig. 5). Results of Fig. 4 and 5 indicate that the power distribution in x-and y-directions are similar and as theory indicates depends on the cross section overlap as obtained by the geometrical optics analysis.

In order to check the validity of Eq. 1 in Fig. 6 expression given by Eq. 1 against d is plotted. The general behavior of the transmission function is very close to the overlap cross section described in theoretical discussion. In Fig. 6, d is the axial offset distance of the source and receiving fiber that can be related to x/y variation in experimental measurements.

To see the effect of the axial serration, z, on the x-and y-scan this separation is increased from the $z = 0.1$ mm (Fig. 4) to 1mm and the transmitted power is shown as a function of x-scan in Fig. 7. Comparing the results of Fig. 4 and 7 two points can be mentioned. First point is

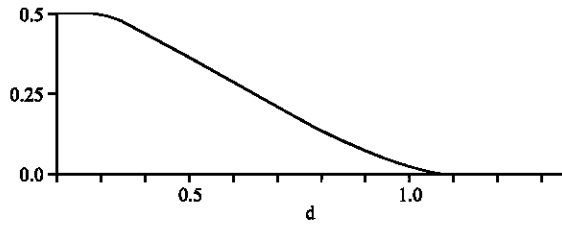


Fig. 6: Variation of the cross section as a function of, d , plotted by Eq. 1

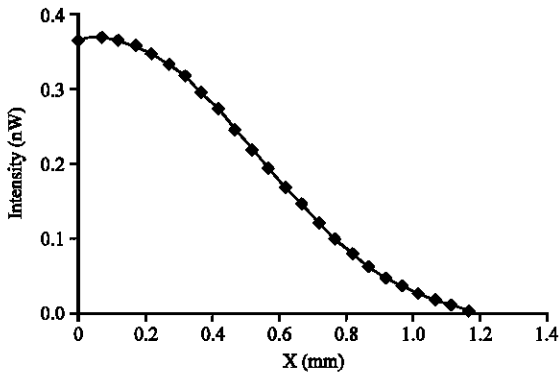


Fig. 7: Intensity variation for x-scan for ($z = 1 \text{ mm}$, $y = 0$)

that by increasing the z value the amount of the transmitted power is reduced in comparison with the previous case ($z = 0.01 \text{ mm}$). Second and perhaps the more important point is that distribution behavior of the transmitted power is changed from a near linear to a nonlinear response as can be shown in Fig. 7. Thus it is concluded that axial separation has influence on the power distribution and one must consider this key point in precise analysis.

Knowing the importance of z variation, in the next study the intensity variation as a function of the air gap variation, z , is investigated and the result is shown in Fig. 8. It is noted that intensity is given by dividing the power by the beam cross section. Looking at Eq. 1, it is noticed that the cross section depends on R^2 value and therefore the intensity curve shows a nonlinear behavior. As shown in Fig. 8, transmitted power generally shows a decrease by an increase in the axial z -value. This power change is from 0.42 nW at z value of about 0.01 mm and drops to 0.07 nW for the $z = 2.6 \text{ mm}$ and for further z value the output is almost constant, which shows the background noise equivalent power. By fitting data points it is noticed that output intensity in z direction changes according to $P_0/(r_1+z\tan\theta)^2$ in which θ is the acceptance angle of the fiber and P_0 is the launched power.

Programs usually use a colormap for the image presentation in color format and for example Matlab uses a colormap, which is a numerical array with three columns

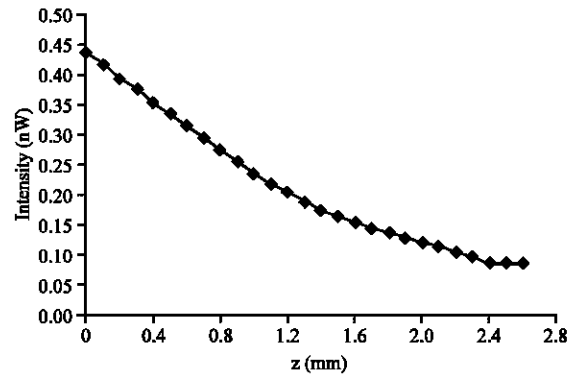


Fig. 8: Intensity variation in receiving fiber in z -scan ($x = 0$, $y = 0$)

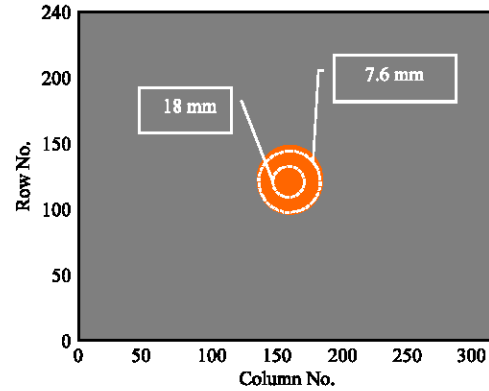


Fig. 9: Comparing images taken at two axial distances ($z = 18 \text{ mm}$, $z = 7.6 \text{ mm}$)

to show color values. This array is called a colormap and each row in the matrix represents individual color using numbers in the range of 0 to 1. The number in each row indicates the intensity of Red, Green and Blue making up a specific color. This method of representation of image is called RGB format. For example for red color the number is (1, 0, 0) and for yellow is (1, 1, 0).

For image analysis, the image of the emerging beam of the source fiber is investigated and such an image is shown in Fig. 9 for two different axial distances. To compare the images, results of two experiments at different z values are obtained separately and then exposed on each other as shown in Fig. 9. The inside circle corresponds to the image case of $z = 18 \text{ mm}$ and outer circle corresponds to z value of 7.6 mm . Details about the image capturing, applications (Awcock and Thomas, 1995) and presentation methods can be found in our recent reports (Golnabi, 2006; Golnabi and Asadpour, 2007). As can be shown in Fig. 9, by using a camera calibration method (He and Li, 2008) one can measure core diameter of the fiber by this technique. Using two images of a single fiber at two distances one is able to

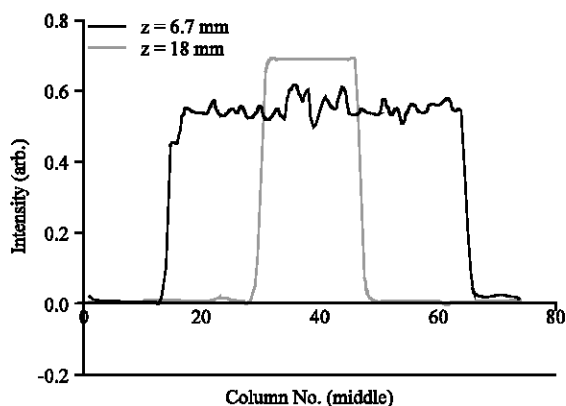


Fig.10: Comparing two image profiles at given axial distances

determine the acceptance angle of the fiber. In our measurements the acceptance angle estimated to be about 0.2° for this particular fiber with a core diameter of about 0.946 mm and white light source. The nominal core diameter for this fiber is 0.860 mm.

In the final study the intensity profile for the transmitted image is obtained by using the image analysis (Golnabi, 2006). We compare two image profiles for given axial distances from fiber end. It is noted that for both axial z values the intensity profile is like a flat-top function. As can be shown in (Fig. 10), a uniform intensity profile is obtained for the given plastic optical fiber illuminated by an incoherent white light.

It shows that output intensity level for the $z = 18$ mm is higher than that of $z = 6.7$ mm (Fig. 10). For a given transmission power since the image cross section for $z = 18$ mm is smaller than for $z = 6.7$ mm thus the intensity for such case is higher, which agrees with the result of Fig. 9. The horizontal scale of Fig. 10 shows the column number related to the data image from CCD to a buffer storage matrix, which has the same order for both functions. As can be seen the transmission function is wider for the case of $z = 6.7$ mm, which corresponds to the larger image circle as shown in Fig. 9 and as a result the transmission function is wider for this image taken at a shorter axial distance from the fiber end.

ACKNOWLEDGMENTS

The Sharif University of Technology Research Program supported this research. The authors like to thank the Research Council for the grant devoted to this project.

REFERENCES

- Awcock, G.J. and R. Thomas, 1995. Applied Image Processing. 1st Edn., Macmillan New Press Ltd., London, ISBN: 0-333-5842-X.
- Cherin, A.H. and P.J. Rich, 1978. Measurement of loss and output numerical aperture of optical fiber splices (E). Applied Opt., 17: 642-645.
- Ersoy, O.K., 2007. Diffraction, Fourier Optics and Imaging. 1st Edn., John Wiley and Sons, Inc., New York., ISBN: 9780471238164.
- Fujii, H., T. Asakura, T. Matsumoto and T. Ohura, 1984. Output power distribution of a large core optical fiber. IEEE J. Lightwave Technol., 2: 1057-1062.
- Golnabi, H., 2006. Precise CCD image analysis for planar laser induced fluorescence experiments. Optics Lasers Technol., 38: 152-161.
- Golnabi, H. and A. Asadpour, 2007. Design and application of industrial vision systems. Robotics Comput. Integrated Manuf., 23: 630-637.
- Golnabi, H. and P. Azimi, 2008. Design and operation of a double-fiber displacement sensor. Optics Commun., 281: 614-620.
- He, B.W. and Y.F. Li, 2008. Camera calibration from vanishing points in a vision system. Optics Lasers Technol., 40: 555-561.
- Heacock, W.D., 1987. Radial image transfer by cylindrical, Step-index optical waveguides. J. Opt. Soc. Am. A, 4: 488-493.
- Raddatz, L., I.H. White, D.G. Cunningham and M.C. Norwell, 1998. An experimental and theoretical study of the offset launch technique for the enhancement of the bandwidth of multimode fiber links. IEEE J. Lightwave Technol., 16: 324-331.
- Ren, D., R. Sharples, J.R. Allington-Smith and G.N. Dodsworth, 2001. Design and construction of a fiber bundle connector using microlenses. Opt. Eng., 40: 2709-2717.
- Senior, J.M., 1992. Optical Fiber Communications. 2nd Prentice Hall International, New York, ISBN: 0-13-635426-2, pp: 281-367.
- Tsekrekos, C.P., R.W. Smink, B.P. De Hon, A.G. Tjihuis and A.M.J. Koonen, 2007. Near-field intensity pattern at the output of silica-based graded-index multimode fibers under selective excitation with a single-mode fiber. Optics Express, 15: 3656-3664.
- Zhang, G., J. He and X. Li, 2005. 3D Vision inspection for internal surface based on circle structured light. Sensor Actuators A, 122: 68-75.